

Teleportation-based noiseless quantum amplification of coherent states of light

JAROMÍR FIURÁŠEK*

Department of Optics, Palacký University, 17. listopadu 1192/12, 771 46 Olomouc, Czech Republic

*fiurasek@optics.upol.cz

Abstract: We propose and theoretically analyze a teleportation-based scheme for high-fidelity noiseless quantum amplification of coherent states of light. In our approach, the probabilistic noiseless quantum amplification operation is encoded into a suitable auxiliary two-mode entangled state and then applied to the input coherent state via continuous-variable quantum teleportation. The scheme requires conditioning on the outcomes of homodyne measurements in the teleportation protocol. In contrast to high-fidelity noiseless quantum amplifiers based on combination of conditional single-photon addition and subtraction, the present scheme requires only photon subtraction in combination with auxiliary Gaussian squeezed vacuum states. We first provide a pure-state description of the protocol which allows us to clearly explain its principles and functioning. Next we develop a more comprehensive model based on phase-space representation of quantum states, that accounts for various experimental imperfections such as excess noise in the auxiliary squeezed states or limited efficiency of the single-photon detectors that can only distinguish the presence or absence of photons. We present and analyze predictions of this phase-space model of the noiseless teleamplifier.

© 2024 Optical Society of America under the terms of the [OSA Open Access Publishing Agreement](#)

1. Introduction

The laws of quantum physics impose fundamental limits on the performance of optical amplifiers. In particular, phase insensitive amplification of light unavoidably adds noise to the amplified signal. This can be understood by observing that the hypothetical noiseless amplification of coherent states $|\alpha\rangle \rightarrow |g\alpha\rangle$ with gain $g > 1$ decreases the overlap between the output states and therefore it cannot be a deterministic physical operation, i.e. a trace-preserving completely positive map. These limits of deterministic amplifiers can be overcome by probabilistic amplifiers [1], where successful amplification is heralded by certain outcome of measurement on an auxiliary quantum system. The probabilistic noiseless amplifiers approximate the (still unphysical) conditional operation $g^{\hat{n}}$, where \hat{n} is the photon number operator, that maps input coherent state $|\alpha\rangle$ onto an amplified coherent state, $\hat{g}^n|\alpha\rangle = e^{(g^2-1)|\alpha|^2/2}|g\alpha\rangle$. The heralded noiseless quantum amplifiers were theoretically proposed by Ralph and Lund [2] and soon afterwards experimentally demonstrated by several groups [3–8]. The probabilistic noiseless quantum amplifiers have attracted significant attention [9–15] because they can be used for suppression of losses in quantum optical communication [16–18], entanglement distillation [19, 20], improvement of continuous-variable quantum teleportation [21], or breeding of larger highly non-classical Schrödinger cat-like states formed by superpositions of coherent states.

The original noiseless quantum amplifier for weak coherent states $|\alpha\rangle$ was based on the modified quantum scissors scheme [22], which truncates the Fock space to the subspace of vacuum and single-photon states. This, however, limits the performance of the amplifier and an amplification gain larger than 1 can be achieved only for coherent states with amplitude $|\alpha| < 0.5$. For larger coherent states one can either split the signal into several modes and utilize several elementary noiseless amplifiers in parallel [2], or consider a generalized quantum scissors scheme with higher Fock-state ancilla $|n\rangle$ [23, 24], which however rapidly increases the experimental complexity of the amplifier. To avoid these drawbacks, an alternative approach to

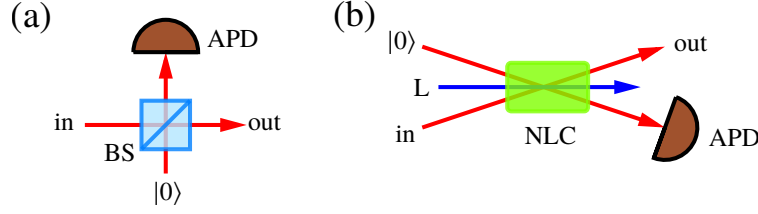


Fig. 1. (a) Conditional single-photon subtraction. BS - highly unbalanced beam splitter with small reflectance $R \ll 1$. APD - single photon detector. (b) Conditional single-photon addition. NLC- nonlinear crystal where the input signal and idler modes are coupled by weak two-mode squeezing interaction. L - pump laser beam. Successful photon addition or subtraction is heralded by click of the detector APD.

noiseless amplification of light was developed based on combination of single-photon addition and subtraction [6, 9, 10]. The resulting conditional noiseless amplifier modulates the amplitudes of Fock states and the full Fock space is preserved. With this approach, high-fidelity noiseless amplification of coherent states is achievable.

The single-photon subtraction can be relatively easily realized by tapping off a small portion of the incoming signal with a highly unbalanced beam splitter with small reflectance $R \ll 1$ and conditioning on detection of a photon in the deflected beam [25–28], see Fig. 1(a). The single-photon addition can be experimentally implemented by injecting the light into the input signal port of a nonlinear crystal that serves as a two-mode squeezer operating in the weak squeezing limit [28, 29], see Fig. 1(b). Conditioning on detection of a photon in the output idler port, we can conclude that a single photon has been coherently added to the signal beam. This scheme has the advantage that inefficient single-photon detection only reduces the success rate but does not reduce the quality of photon addition operation, provided that the nonlinear interaction in the crystal is sufficiently weak.

The photon addition is much more experimentally demanding than photon subtraction and one can ask if a noiseless quantum amplifier can be designed where photon addition is avoided and only photon subtraction is employed. It was proposed and experimentally demonstrated that one can approximate noiseless amplification by random displacements of the input coherent state followed by subtraction of several photons from the displaced state. This works because the photon subtraction happens with highest probability if the random displacement occurs in the direction of the input coherent state [5, 10]. However, this process does add some noise to the output state. Here we are interested in implementation of a truly noiseless amplifier, that under perfect circumstances conditionally transforms pure input coherent states $|\alpha\rangle$ onto pure output states closely approximating $|g\alpha\rangle$.

In the present paper, we exploit the concept of teleportation of quantum gates [30] to design a noiseless quantum amplifier based on auxiliary Gaussian squeezed states and photon subtraction. The conditional noiseless amplification operation is encoded into suitably modified entangled two-mode squeezed vacuum state that serves as a quantum channel in continuous-variable quantum teleportation [31]. In contrast to ordinary deterministic quantum teleportation, we must condition on the outcomes of homodyne measurements in the teleportation protocol [32] to achieve noiseless amplification. In this setting we can avoid the photon addition operation because, due to the perfect photon number correlations between the signal and idler modes of two-mode squeezed vacuum, addition of a photon to the signal mode becomes equivalent to photon subtraction from the idler mode. We thus replace the photon addition operation with an ancilla two-mode entangled state that can be prepared from Gaussian two-mode squeezed vacuum states by conditional photon subtractions.

Previous works have investigated entanglement distillation by noiseless amplification of the two-mode squeezed vacuum state and the improvement of continuous-variable teleportation by utilizing the noiselessly amplified two-mode squeezed vacuum state as a quantum channel in teleportation [19–21]. Here, we make important step further beyond these previous studies and use the continuous-variable quantum teleportation scheme for conditional noiseless amplification of the teleported state. We note that also the noiseless quantum amplifier based on the quantum scissors scheme can be interpreted as a quantum tele-amplifier, that requires ancilla Fock states and is driven by projection on a suitable multimode n -photon state [24].

The rest of the present paper is organized as follows. In Section 2 we present a pure-state description of the protocol which allows us to easily explain its main working principles. Subsequently, in Section 3 we develop a more realistic model of the teleportation-based noiseless amplifier that takes into account the various experimental imperfections. This model is based on the powerful and well established phase-space techniques, where the states are represented by their Wigner functions or Husimi Q -functions. Finally, Section 4 contains a brief summary and conclusions.

2. Teleportation-based noiseless quantum amplifier

We start with a brief overview of the probabilistic noiseless amplification of coherent states via combination of conditional single-photon addition and subtraction. The simplest instance of such noiseless quantum amplifier consists of single-photon addition followed by single-photon subtraction [6, 9, 10], described by the operator

$$\hat{a}\hat{a}^\dagger = \hat{n} + 1, \quad (1)$$

where \hat{a} and \hat{a}^\dagger denote the annihilation and creation operators and \hat{n} stands for the photon number operator. For the sake of presentation simplicity, we neglect here for the moment the effects of the reflectance R of the tapping beam splitter in the photon subtraction and the finite squeezing in the nonlinear crystal utilized in the photon addition. For weak coherent states with $|\alpha| \ll 1$ we can write $|\alpha\rangle \approx |0\rangle + \alpha|1\rangle$ and after the conditional amplification we get

$$(\hat{n} + 1)(|0\rangle + \alpha|1\rangle) = |0\rangle + 2\alpha|1\rangle, \quad (2)$$

hence the state is amplified with amplitude gain $g = 2$. More generally, we can consider a coherent superposition of single-photon addition followed by single-photon subtraction and single-photon subtraction followed by single-photon addition [9],

$$\hat{G} = \hat{a}\hat{a}^\dagger + (g - 2)\hat{a}^\dagger\hat{a}. \quad (3)$$

This amplifier achieves gain g for weak coherent states, $\hat{G}(|0\rangle + \alpha|1\rangle) = |0\rangle + g\alpha|1\rangle$. The conditional operation (3) can be realized with an interferometric scheme, where photon subtraction is attempted both before and after the photon addition and the two subtracted beams are overlapped on a beam splitter before detecting the subtracted photon [33, 34]. This erases the which way information about the origin of the subtracted photon and produces the coherent superposition (3), where the relative weight of the terms $\hat{a}\hat{a}^\dagger$ and $\hat{a}^\dagger\hat{a}$ can be controlled by the splitting ratio of the beam splitter where the two subtracted beams interfere.

The conditional photon addition is experimentally much more challenging than the photon subtraction. Moreover, in experiments with continuous signals, the photon subtraction is well mastered, while the conditional photon addition to a specific temporal mode may be difficult to accomplish. It is therefore worth asking whether the photon addition could be replaced by photon subtraction and other accessible resources. In this paper we answer this question in affirmative by proposing a teleportation-based noiseless quantum amplifier. Our approach requires auxiliary

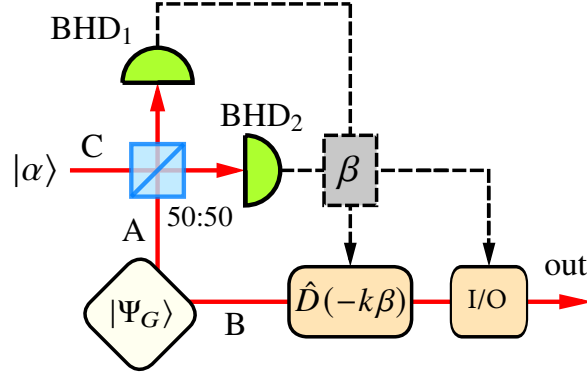


Fig. 2. Teleportation-based noiseless quantum amplifier. Modes A and B are prepared in a suitable entangled state $|\Psi_G\rangle$ that encodes the amplification operation \hat{G} . The input coherent state is injected in mode C . Modes A and C interfere on balanced beam splitter and are measured with two balanced homodyne detectors BHD. Mode B can be coherently displaced and the output state is accepted or rejected depending on the measurement outcome β .

Gaussian squeezed states, but it does not require auxiliary single-photon states and we avoid injection and mode-matching of the amplified signal beam in a nonlinear crystal. Specifically, we can imprint the conditional operation \hat{G} into a two-mode squeezed vacuum state

$$|\Psi(\lambda)\rangle = \sqrt{1-\lambda^2} \sum_{n=0}^{\infty} \lambda^n |n, n\rangle, \quad (4)$$

and use the modified state

$$|\Psi_G(\lambda)\rangle = \frac{1}{\sqrt{P_G}} \hat{I} \otimes \hat{G} |\Psi(\lambda)\rangle \quad (5)$$

as a quantum channel in continuous-variable quantum teleportation. Here

$$P_G = \langle \Psi(\lambda) | \hat{I} \otimes \hat{G}^\dagger \hat{G} | \Psi(\lambda) \rangle \quad (6)$$

is a normalization factor and \hat{I} denotes a single-mode identity operator. We utilize the standard Braunstein-Kimble teleportation protocol [31], see Fig. 2. The teleported state is combined on a balanced beam splitter with one part of the two-mode entangled state (5) and two homodyne detectors measure the amplitude quadrature \hat{x}_1 of the first output mode and the phase quadrature \hat{p}_2 of the second output mode, yielding a complex output signal $\beta = x_1 + ip_2$. In a deterministic protocol, Bob coherently displaces his mode depending on the measurement outcome β to conclude the teleportation. However, when we use the modified state $|\Psi_G(\lambda)\rangle$ for teleportation-based noiseless amplification we need to condition on outcomes β close to $\beta = 0$ because the operator \hat{G} does not commute with the displacement operator. Since the state $|\Psi_G(\lambda)\rangle$ can be prepared before any attempted noiseless amplification, the probabilistic nature of the noiseless amplification in this teleportation protocol is solely due to conditioning on the selected range of measurement outcomes β .

We observe that for $\beta = 0$ the noiseless amplification is implemented perfectly up to an additional attenuation due to finite squeezing, i.e. the output state is $\hat{G}|\lambda\alpha\rangle$ for any input state $|\alpha\rangle$. To see this, define a non-normalized infinitely squeezed state

$$|\Psi_{\text{EPR}}\rangle = \frac{1}{\sqrt{\pi}} \sum_{n=0}^{\infty} |n, n\rangle. \quad (7)$$

For $\beta = 0$, the modes A and C in Fig. 2 are projected on state $|\Psi_{\text{EPR}}\rangle$, and the teleported state can be expressed as

$$|\varphi\rangle_B = {}_{AC}\langle\Psi_{\text{EPR}}|\Psi_G(\lambda)\rangle_{AB}|\alpha\rangle_C. \quad (8)$$

Taking into account the perfect photon number correlations in states $|\Psi(\lambda)\rangle$ and $|\Psi_{\text{EPR}}\rangle$ and expanding the coherent state $|\alpha\rangle$ in Fock basis,

$$|\alpha\rangle = e^{-|\alpha|^2/2} \sum_{n=0}^{\infty} \frac{\alpha^n}{\sqrt{n!}} |n\rangle, \quad (9)$$

we find after some algebra that

$$|\varphi\rangle = \sqrt{\frac{1-\lambda^2}{\pi P_G}} e^{-(1-\lambda^2)|\alpha|^2/2} \hat{G}|\lambda\alpha\rangle. \quad (10)$$

We can see that the effective amplification gain is reduced by the finite squeezing strength $\lambda < 1$, $g_{\text{eff}} = \lambda g$. The performance of the conditional noiseless amplifier can be more comprehensively characterized by the actual amplitude dependent amplification gain

$$g(\alpha) = \frac{1}{\alpha} \frac{\langle\varphi|\hat{a}|\varphi\rangle}{\langle\varphi|\varphi\rangle} = \lambda + \frac{\lambda(g-1)[1+(g-1)|\lambda\alpha|^2]}{[1+(g-1)|\lambda\alpha|^2]^2 + (g-1)^2|\lambda\alpha|^2} \quad (11)$$

and the fidelity of the output state $|\varphi\rangle$ with the amplified coherent state $|g\lambda\alpha\rangle$,

$$\mathcal{F}(\alpha) = \frac{|\langle\varphi|g\lambda\alpha\rangle|^2}{\langle\varphi|\varphi\rangle} = \frac{[1+g(g-1)|\lambda\alpha|^2]^2}{[1+(g-1)|\lambda\alpha|^2]^2 + (g-1)^2|\lambda\alpha|^2} e^{-(g-1)^2|\lambda\alpha|^2}. \quad (12)$$

Let us now discuss the preparation of the resource entangled state (5). Consider first the noiseless amplification via the conditional operation (1). The target entangled state reads

$$\hat{b}\hat{b}^\dagger|\Psi(\lambda)\rangle_{AB} = \sqrt{1-\lambda^2} \sum_{n=0}^{\infty} (n+1)\lambda^n |n, n\rangle_{AB}. \quad (13)$$

Remarkably, this state can be obtained by subtracting a single photon from each mode of the two-mode squeezed vacuum state [35],

$$\hat{a}\hat{b}|\Psi(\lambda)\rangle_{AB} = \lambda\sqrt{1-\lambda^2} \sum_{n=0}^{\infty} (n+1)\lambda^n |n, n\rangle_{AB}. \quad (14)$$

Due to the perfect photon number correlations between the two modes the addition of a photon to mode B becomes equivalent to subtraction of a photon from mode A . The joint subtraction of two photons from a two-mode squeezed vacuum state has already been successfully demonstrated experimentally [36, 37]. For weakly squeezed states, the local photon subtractions can conditionally increase the entanglement of the state and can thus serve for continuous-variable entanglement distillation.

Consider now preparation of the resource state $|\Psi_G(\lambda)\rangle$ for the more general noiseless amplification operation \hat{G} given by Eq. (3). We have

$$[\hat{b}\hat{b}^\dagger + (g-2)\hat{b}^\dagger\hat{b}]|\Psi(\lambda)\rangle_{AB} = \sqrt{1-\lambda^2} \sum_{n=0}^{\infty} [(g-1)n+1]\lambda^n |n, n\rangle. \quad (15)$$

This state can be prepared from a two-mode squeezed vacuum state by a modified joint photon subtraction from each mode, where an auxiliary weak two-mode squeezed vacuum state is

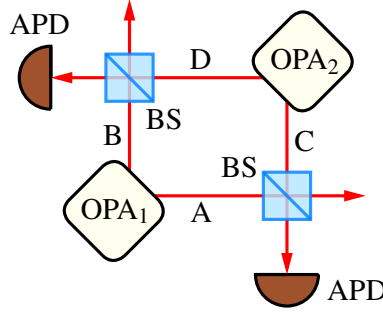


Fig. 3. Preparation of entangled state for teleportation-based noiseless amplification via generalized photon subtraction [38]. The optical parametric amplifiers OPA generate two-mode squeezed vacuum states with different squeezing strengths λ and μ . The squeezed states interfere on beam splitters BS and the output modes C and D are measured with single photon detectors APD. Successful state preparation is heralded by simultaneous click of both detectors APD.

injected into the auxiliary input ports of the beam splitters that serve for photon subtraction [38]. The scheme is illustrated in Fig. 3 and the successful state preparation is heralded by simultaneous click of both single-photon detectors APD. Let us assume that perfect photon number resolving detectors are employed that project the output modes C and D on single-photon Fock states $|1, 1\rangle_{CD}$. Let μ denote the squeezing strength of the auxiliary two-mode squeezed vacuum state $|\Psi(\mu)\rangle_{CD}$ and let $T = 1 - R$ denote the intensity transmittance of the two tapping beam splitters BS in Fig. 3. The conditionally prepared state of modes A and B can be expressed as

$$|\Psi_G\rangle_{AB} = \frac{\sqrt{1-\lambda^2}\sqrt{1-\mu^2}}{\sqrt{P_S}} \sum_{n=0}^{\infty} (T\lambda + R\mu)^{n-1} [nRT(\lambda - \mu)^2 + (R\lambda + T\mu)(T\lambda + R\mu)] |n, n\rangle, \quad (16)$$

where

$$P_S = \frac{(1-\lambda^2)(1-\mu^2)}{(1-\lambda_{\text{eff}}^2)^3} \left\{ [(1-\lambda_{\text{eff}}^2)(R\lambda + T\mu) - \lambda_{\text{eff}}RT(\lambda - \mu)^2]^2 + R^2T^2(\lambda - \mu)^4 \right\} \quad (17)$$

is the probability of successful joint conditional single-photon subtraction. The state (16) is exactly of the form (15), with the effective two-mode squeezing constant

$$\lambda_{\text{eff}} = T\lambda + R\mu, \quad (18)$$

nominal amplification gain

$$g = 1 + \frac{RT(\lambda - \mu)^2}{(R\lambda + T\mu)(R\mu + T\lambda)}, \quad (19)$$

and a resulting effective amplification gain $g_{\text{eff}} = \lambda_{\text{eff}}g$.

The experimentally available single-photon detectors usually only distinguish the presence or absence of photons but do not resolve their number. Moreover, the detectors have only limited detection efficiency η . The photon subtraction scheme shown in Fig. 3 can faithfully generate the desired target state (15) even under such imperfect experimental conditions provided that the beam splitters BS are highly unbalanced and the auxiliary input state $|\Psi(\mu)\rangle_{CD}$ is only very weakly squeezed,

$$|\mu|^2 \ll R \ll 1. \quad (20)$$

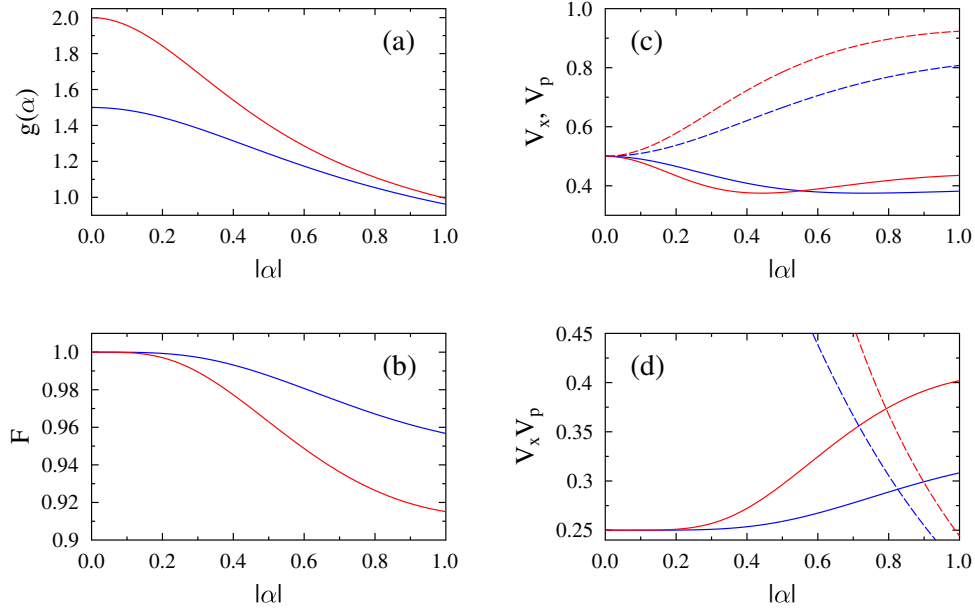


Fig. 4. Performance of teleportation-based noiseless quantum amplification of coherent states $|\alpha\rangle$ with pure resource entangled state (15) with $\lambda = 0.5$. The results are plotted for two different effective gains $g_{\text{eff}} = 2$ (red lines) and $g_{\text{eff}} = 1.5$ (blue lines). Projection on $\beta = 0$ is assumed in the teleportation protocol. (a) The amplitude-dependent amplification gain $g(\alpha)$. (b) Fidelity of the amplified state with coherent state $|g(\alpha)\alpha\rangle$. (c) Variances V_x (solid lines) and V_p (dashed lines) of the amplitude and phase quadratures of the amplified state. (d) The uncertainty product $V_x V_p$. The dashed lines show the uncertainty product for the optimal linear deterministic amplifier: $g^2(\alpha)/2 - 1/4$.

Under this condition, the auxiliary input state of modes C and D can be approximated as $|0, 0\rangle + \mu|1, 1\rangle$. The two dominant events leading to the simultaneous clicks of the two detectors APD in Fig. 3 are that either the auxiliary modes C and D are in vacuum state and a single photon is subtracted from both input modes A and B (probability scaling R^2), or that a single photon is present in each of the auxiliary input modes C and D and these photons are transmitted through the beam splitters BS and detected by APDs (probability scaling $|\mu|^2$). The dominant unwanted event where one photon is subtracted from mode A and the other APD is triggered by a photon present in the input mode D has a probability that scales as $R|\mu|^2$, which is much smaller than the probability of the desired events provided that the inequality (20) holds. A detailed analysis of the whole teleportation-based noiseless amplifier that takes into account these experimental limitations is provided in the next section. Here we just note that in the limit $|\mu| \ll 1$ and $R \ll 1$ the expression for the effective gain simplifies and we can write

$$g_{\text{eff}} \approx T\lambda \left(1 + \frac{R\lambda}{R\lambda + T\mu} \right). \quad (21)$$

Note that μ and λ can have opposite signs and therefore the effective gain g_{eff} can be arbitrarily high. We observe that the effective amplification gain is rather sensitive to small changes of μ . To see this explicitly, we evaluate $dg_{\text{eff}}/d\mu$ and obtain

$$\frac{dg_{\text{eff}}}{d\mu} = 2R - \frac{R\lambda^2}{(R\lambda + T\mu)^2} = 2R - \frac{\lambda^2(g_{\text{eff}} - \lambda_{\text{eff}})^2}{RT^2(\lambda - \mu)^4}. \quad (22)$$

For typical configurations with $R \ll 1$ and $|\mu| \ll |\lambda|$ we find that $dg_{\text{eff}}/d\mu \approx -(g_{\text{eff}} - \lambda_{\text{eff}})^2/(\lambda^2 R)$. Especially achieving large effective gains g_{eff} requires destructive quantum interference, i.e. $\lambda > 0$ and $\mu < 0$, and the resulting small term $R\lambda + T\mu$ in the denominator of Eqs. (19) and (21) implies high sensitivity of g_{eff} to changes of μ .

Figure 4 illustrates the performance of teleportation-based noiseless quantum amplifier for two different gains. We consider noiseless amplification with pure entangled state (15) and conditioning on $\beta = 0$, which leads to the best possible performance of the amplifier. The results depicted in Fig. 4 thus provide a benchmark for comparison with predictions of more realistic models discussed in the next section. For small $|\alpha|$, the noiseless amplification is practically perfect. For larger $|\alpha|$, the resulting amplification gain and fidelity begins to decrease and the uncertainty product $V_x V_p$ grows, indicating that the amplified state is no longer a minimum uncertainty state. Note that a deterministic amplifier would result in an uncertainty product $V_x V_p = g^2(\alpha)/2 - 1/4$, indicated by dashed lines in Fig. 4(d).

The conditional operation (3) approximates the noiseless amplifier well only for relatively weak coherent states with $|\alpha| < 1$. Better approximation can be achieved with more sophisticated filters that approximate the unphysical operation $g^{\hat{n}}$ on a larger subspace of the Fock states. In particular, one can consider the following operation where the amplification is truncated at Fock state $|N\rangle$ [1, 15, 19],

$$\hat{G}_N = \frac{1}{g^N} \sum_{n=0}^N g^n |n\rangle\langle n| + \sum_{n=N+1}^{\infty} |n\rangle\langle n|. \quad (23)$$

The corresponding normalized resource entangled state for teleportation-based noiseless amplification reads

$$|\Psi_N(\lambda)\rangle = \sqrt{\frac{1-\lambda^2}{P_N}} \left[\frac{1}{g^N} \sum_{n=0}^N (g\lambda)^n |n, n\rangle + \sum_{n=N+1}^{\infty} \lambda^n |n, n\rangle \right], \quad (24)$$

where

$$P_N = \frac{1}{g^{2N}} \frac{1-\lambda^2}{1-g^2\lambda^2} \left[1 - (g\lambda)^{2N+2} \right] + \lambda^{2N+2} \quad (25)$$

is a normalization factor. With the resource state (24) it is possible to achieve essentially perfect probabilistic noiseless amplification with finite probability $P_{\text{tele}} > 0$ for a range of coherent states with $|\alpha| < |\alpha_{\text{th}}|$. The threshold amplitude α_{th} can be estimated from the requirement that the effective support of the amplified coherent state $|g\lambda\alpha_{\text{th}}\rangle$ falls within the subspace spanned by the first $N+1$ Fock states. We quantify the width of the coherent state in Fock basis by three standard deviations of its photon number distribution. This yields $g^2\lambda^2|\alpha_{\text{th}}|^2 + 3g\lambda|\alpha_{\text{th}}| = N$ and, consequently

$$|\alpha_{\text{th}}| = \frac{1}{g\lambda} \left(\sqrt{N + \frac{9}{4}} - \frac{3}{2} \right). \quad (26)$$

As a preparatory step for further discussion let us recall some facts about the continuous-variable teleportation of coherent states in the Braunstein-Kimble scheme [31]. The measurement outcome β indicates that the modes A and C were projected onto coherently displaced EPR state $\hat{I}_A \otimes \hat{D}_C(\beta^*) |\Psi_{\text{EPR}}\rangle_{AC}$, where $\hat{D}(\beta) = \exp(\hat{a}^\dagger \beta - \hat{a} \beta^*)$. This can be equivalently interpreted as a coherent displacement of the input state in mode C , $\hat{D}(\beta) |\alpha\rangle_C = |\alpha + \beta\rangle_C$, followed by projection of modes A and C onto the EPR state $|\Psi_{\text{EPR}}\rangle$. This in turn is equivalent to the projection of mode A onto the re-normalized coherent state $\frac{1}{\sqrt{\pi}} |\alpha^* + \beta^*\rangle$. The measurement outcomes β span the whole complex plane and the overcompleteness of projectors onto coherent states is accounted for by the prefactor $1/\sqrt{\pi}$ in our definition of the EPR state $|\Psi_{\text{EPR}}\rangle$, which ensures that we obtain correct probability density of measurement outcomes.

Let us first consider teleportation with the Gaussian two-mode squeezed vacuum state (4). Conditional on measurement outcome β , which occurs with probability density

$$P(\beta) = \frac{1}{\pi} (1 - \lambda^2) e^{-(1-\lambda^2)|\alpha+\beta|^2}, \quad (27)$$

the mode B is prepared in a coherent state $|\lambda\alpha + \lambda\beta\rangle$. If a corrective displacement operation $\hat{D}(-\lambda\beta)$ is applied to mode B , the teleported state becomes $|\lambda\alpha\rangle$, irrespective of the measurement outcome β . The teleportation thus becomes equivalent to a purely lossy channel with amplitude transmittance λ [32]. This should be contrasted with the unity gain teleportation, where the corrective displacement operation reads $\hat{D}(-\beta)$ and the output state becomes a thermal displaced state with coherent amplitude α and added thermal noise.

Let us now turn to teleportation with the entangled state (24). If the coherent amplitude $\alpha + \beta$ satisfies the condition

$$|\alpha + \beta| < |\alpha_{\text{th}}|, \quad (28)$$

then the tail of the entangled state $|\Psi_N(\lambda)\rangle$ represented by the second sum in the formula (24) becomes irrelevant and the output state conditional on measurement outcome β will be the noiselessly amplified coherent state $|g\lambda\alpha + g\lambda\beta\rangle$. After correcting displacement operation $\hat{D}(-g\lambda\beta)$ we recover the noiselessly amplified input state $|g\lambda\alpha\rangle$. The probability density of the measurement outcomes β can be expressed as

$$P(\beta) = \frac{1}{\pi} \frac{1 - \lambda^2}{g^{2N} P_N} e^{(g^2 \lambda^2 - 1)|\alpha+\beta|^2}, \quad (29)$$

which is valid for β that satisfy the inequality (28). In order to satisfy the condition (28) for some chosen range of input coherent amplitudes α the outcome of the teleportation-based amplifier is accepted only if $|\beta|$ is smaller than some threshold σ . In order to obtain analytical expression for the resulting success probability P_{tele} , we can instead assume that the outcome β is accepted with probability $\exp(-|\beta|^2/\sigma^2)$ and rejected otherwise. We have

$$P_{\text{tele}} = \int_{\beta} P(\beta) e^{-\frac{|\beta|^2}{\sigma^2}} d^2\beta, \quad (30)$$

which yields

$$P_{\text{tele}} = \frac{1 - \lambda^2}{g^{2N} P_N} \frac{\sigma^2}{1 + \sigma^2 - \sigma^2 \lambda^2 g^2} \exp \left[\frac{(\lambda^2 g^2 - 1)|\alpha|^2}{1 + \sigma^2 - \sigma^2 \lambda^2 g^2} \right]. \quad (31)$$

This formula is meaningful only if σ and $|\alpha|$ are sufficiently small such that the following conditions are satisfied

$$\sigma^2 < \frac{1}{\lambda^2 g^2 - 1}, \quad \frac{\lambda g |\alpha|}{1 + \sigma^2 - \sigma^2 \lambda^2 g^2} + \frac{3 \lambda g \sigma}{\sqrt{2(\sigma^2 + 1 - \sigma^2 \lambda^2 g^2)}} < \sqrt{N + \frac{9}{4}} - \frac{3}{2}. \quad (32)$$

The first inequality ensures that the Gaussian integral in (30) converges and the second inequality guarantees that the range of complex amplitudes β that non-negligibly contribute to the integral (30) includes only β for which the condition (28) is satisfied. The factor 3 appearing in Eq. (32) means that we take three standard deviations as the effective width of the involved Gaussian distribution of β .

3. Phase-space description of teleportation-based noiseless quantum amplifier

In this section we present results of a more realistic model of the teleportation-based noiseless quantum amplifier that takes into account the main experimental imperfections. The model is

based on the well-established phase-space approach, where the Wigner function of a non-Gaussian state generated by photon subtractions from some Gaussian state can be expressed as a linear combination of several Gaussian Wigner functions [39, 40]. Here we choose to work with the Husimi Q -function instead of the Wigner function, because with the Q -function it is particularly straightforward to calculate projections onto coherent states. Let us begin with some useful definitions. we consider system of N modes, we denote by \hat{x}_j and \hat{p}_j the amplitude and phase quadrature operators of the j th mode, respectively, and we collect the quadrature operators into a vector $\hat{\mathbf{q}} = (\hat{x}_1, \hat{p}_1, \dots, \hat{x}_N, \hat{p}_N)^T$. The covariance matrix γ of the state is a $2N \times 2N$ square matrix with elements

$$\gamma_{jk} = \langle \Delta \hat{q}_j \Delta \hat{q}_k + \Delta \hat{q}_k \Delta \hat{q}_j \rangle. \quad (33)$$

where $\Delta \hat{q}_j = \hat{q}_j - \langle \hat{q}_j \rangle$. In particular, a covariance matrix of a two-mode squeezed vacuum state (4) with $\lambda = \tanh r$, where r is the squeezing constant, reads

$$\gamma_{\text{TMSV}}(r) = \begin{pmatrix} \cosh(2r) & 0 & \sinh(2r) & 0 \\ 0 & \cosh(2r) & 0 & -\sinh(2r) \\ \sinh(2r) & 0 & \cosh(2r) & 0 \\ 0 & -\sinh(2r) & 0 & \cosh(2r) \end{pmatrix}. \quad (34)$$

Note that the covariance matrix of vacuum state is equal to the identity matrix, $\gamma_{\text{vac}} = I$.

Let us first describe the preparation of the two-mode resource state (15) according to the scheme shown in Fig. 3. Our model assumes that the input states of modes A, B and C, D are Gaussian noisy two-mode squeezed thermal states that can be equivalently represented as initial pure two-mode squeezed states transmitted through a lossy channel with some effective transmittance η . The covariance matrices of the resulting mixed Gaussian states read

$$\gamma_{\text{AB}}^{\text{in}} = \eta_{\text{AB}} \gamma_{\text{TMSV}}(r) + (1 - \eta_{\text{AB}})I, \quad \gamma_{\text{CD}}^{\text{in}} = \eta_{\text{CD}} \gamma_{\text{TMSV}}(s) + (1 - \eta_{\text{CD}})I, \quad (35)$$

where r and s denote the bare squeezing constants of the initial pure states before losses, and $\mu = \tanh s$. The parametrization in terms of effective losses is experimentally intuitive because it corresponds to a picture where the source generates pure states that are affected by losses both in the source and during the subsequent signal transmission.

The single-photon detectors APD in Fig. 3 are modeled as on-off detectors that can only distinguish the presence or absence of photons and have overall detection efficiency η_{APD} . It is convenient to account for the inefficient detection by letting the detected modes propagate through a lossy channel with transmittance η_{APD} followed by perfect on-off detectors whose click is described by POVM element $\hat{I} - |0\rangle\langle 0|$. In the state preparation scheme shown in Fig. 3 we condition on simultaneous clicks of both APDs and the corresponding POVM element therefore reads

$$\hat{\Pi}_{\text{CD}} = (\hat{I} - |0\rangle\langle 0|)_C \otimes (\hat{I} - |0\rangle\langle 0|)_D. \quad (36)$$

The effective covariance matrix of the overall Gaussian state of the four modes A, B, C, D just before the measurement on modes C and D can be expressed as

$$\gamma_{\text{eff,ABCD}} = S_{\text{APD}} S_{\text{BS}} (\gamma_{\text{AB}}^{\text{in}} \oplus \gamma_{\text{CD}}^{\text{in}}) S_{\text{BS}}^T S_{\text{APD}}^T + G_{\text{APD}}, \quad (37)$$

where

$$S_{\text{PD}} = I_{\text{AB}} \oplus \sqrt{\eta_{\text{PD}}} I_{\text{CD}}, \quad G_{\text{PD}} = 0_{\text{AB}} \oplus (1 - \eta_{\text{PD}}) I_{\text{CD}}, \quad (38)$$

represent the effective lossy channels in modes C and D that account for inefficient single-photon detection, and S_{BS} is a symplectic matrix that describes the coupling of modes A, C and B, D at the two beam splitters BS with transmittance T and reflectance R .

The Husimi Q -function of a two-mode state $\hat{\rho}_{AB}$ is defined as

$$Q(\omega_A, \omega_B) = \frac{1}{\pi^2} \langle \omega_A, \omega_B | \hat{\rho}_{AB} | \omega_A, \omega_B \rangle, \quad (39)$$

where $|\omega_A, \omega_B\rangle$ denotes a coherent state of modes A and B with complex amplitudes ω_A and ω_B , respectively. For Gaussian states $\hat{\rho}$ the Q -function (39) is a Gaussian distribution. The POVM (36) is a linear combination of four projectors onto Gaussian states. Therefore, the Husimi Q -function of the conditionally generated state of modes A and B can be expressed as linear combination of four Gaussian states [41],

$$Q_{AB}(\omega_A, \omega_B) = \frac{1}{P_{AB}} \sum_{j=1}^4 C_j \sqrt{\frac{\det \tilde{\Gamma}_j}{\det \Gamma_j}} \frac{\sqrt{\det \Gamma_j}}{\pi^2} e^{-\mathbf{r}_\omega^T \Gamma_j \mathbf{r}_\omega}, \quad (40)$$

where $C_1 = C_4 = 1$, $C_2 = C_3 = 1$, and $\mathbf{r}_\omega = [\text{Re}(\omega_A), \text{Im}(\omega_A), \text{Re}(\omega_B), \text{Im}(\omega_B)]^T$ is a real vector composed of real and imaginary parts of the complex amplitudes ω_A and ω_B . The matrices $\tilde{\Gamma}_j$ have different sizes and are related to input covariance matrices of modes AB , ABC , ABD , and $ABCD$, respectively,

$$\begin{aligned} \tilde{\Gamma}_1 &= 2(\gamma_{\text{eff},AB} + I)^{-1}, & \tilde{\Gamma}_2 &= 2(\gamma_{\text{eff},ABC} + I)^{-1}, \\ \tilde{\Gamma}_3 &= 2(\gamma_{\text{eff},ABD} + I)^{-1}, & \tilde{\Gamma}_4 &= 2(\gamma_{\text{eff},ABCD} + I)^{-1}. \end{aligned} \quad (41)$$

Here the two-mode and three-mode covariance matrices $\gamma_{\text{eff},AB}$, $\gamma_{\text{eff},ABC}$ and $\gamma_{\text{eff},ABD}$ are submatrices of the full covariance matrix (37). The matrices Γ_j appearing in the exponent in Eq. (40) are then extracted from $\tilde{\Gamma}_j$ as two-mode submatrices corresponding to modes A and B . Note that, in particular, $\Gamma_1 = \tilde{\Gamma}_1$. Finally, the probability P_{AB} of conditional state preparation is given by

$$P_{AB} = \sum_{j=1}^4 C_j \sqrt{\frac{\det \tilde{\Gamma}_j}{\det \Gamma_j}}. \quad (42)$$

With the phase-space representation of the resource entangled state we can proceed to analysis of the teleportation-based noiseless amplification of coherent states $|\alpha\rangle$. As discussed in the previous section, the teleported state corresponding to measurement outcome β can be obtained by projecting the mode A of the two-mode entangled state (40) onto the re-normalized coherent state $\frac{1}{\sqrt{\pi}}|\alpha^* + \beta^*\rangle$. We introduce two real displacement vectors

$$\mathbf{d}_\alpha = [\text{Re}(\alpha), \text{Im}(\alpha)]^T, \quad \mathbf{d}_\beta = [\text{Re}(\beta), \text{Im}(\beta)]^T. \quad (43)$$

To illustrate the calculations, consider teleportation with a generic two-mode Gaussian state with Q -function

$$Q(\omega_A, \omega_B) = \frac{\sqrt{\det \Gamma}}{\pi^2} e^{-\mathbf{r}_\omega^T \Gamma \mathbf{r}_\omega}. \quad (44)$$

We introduce a bipartite $A|B$ splitting of the matrix Γ ,

$$\Gamma = \begin{pmatrix} \Gamma_A & M \\ M^T & \Gamma_B \end{pmatrix}. \quad (45)$$

The Q -function of a non-normalized state of mode B corresponding to projection of mode A onto $\frac{1}{\sqrt{\pi}}|\alpha^* + \beta^*\rangle$ reads

$$Q_B(\omega_B|\beta) = \frac{\sqrt{\det \Gamma}}{\pi^2} \exp \left(-\mathbf{r}_{\omega_B}^T \Gamma_B \mathbf{r}_{\omega_B} - \mathbf{d}^T \Upsilon^T M \mathbf{r}_{\omega_B} - \mathbf{r}_{\omega_B}^T M^T \Upsilon \mathbf{d} - \mathbf{d}^T \Upsilon^T \Gamma_A \Upsilon \mathbf{d} \right), \quad (46)$$

where $\mathbf{d} = \mathbf{d}_\alpha + \mathbf{d}_\beta$, $\mathbf{r}_{\omega_B} = [\text{Re}(\omega_B), \text{Im}(\omega_B)]^T$, and the matrix

$$\Upsilon = \begin{pmatrix} 1 & 0 \\ 0 & -1 \end{pmatrix} \quad (47)$$

accounts for the complex conjugation of α and β . Specifically, for $\beta = 0$ we get

$$\mathcal{Q}_B(\omega_B|\beta=0) = K(\alpha) \frac{\sqrt{\det \Gamma_B}}{\pi} \exp \left[-(\mathbf{r}_{\omega_B} - D\mathbf{d}_\alpha)^T \Gamma_B (\mathbf{r}_{\omega_B} - D\mathbf{d}_\alpha) \right], \quad (48)$$

where

$$K(\alpha) = \frac{1}{\pi} \sqrt{\frac{\det \Gamma}{\det \Gamma_B}} e^{-\mathbf{d}_\alpha^T \tilde{\Gamma}_A \mathbf{d}_\alpha}, \quad (49)$$

and

$$\tilde{\Gamma}_A = \Upsilon^T \Gamma_A \Upsilon - \Upsilon^T M \Gamma_B^{-1} M^T \Upsilon, \quad D = -\Gamma_B^{-1} M^T \Upsilon. \quad (50)$$

The output Gaussian state (48) has covariance matrix $\gamma_B = 2\Gamma_B^{-1} - I$ and coherent displacement $D\mathbf{d}_\alpha$.

Let us now turn to teleportation with a non-Gaussian entangled resource state (40). We can write the normalized output teleported state conditioned on $\beta = 0$ as a linear combination of four Gaussian states,

$$\mathcal{Q}_B(\omega_B|\beta=0) = \frac{1}{P_0} \sum_{j=1}^4 C_j \tilde{K}_j(\alpha) \frac{\sqrt{\det \Gamma_{B,j}}}{\pi} e^{-(\mathbf{r}_{\omega_B} - D_j \mathbf{d}_\alpha)^T \Gamma_{B,j} (\mathbf{r}_{\omega_B} - D_j \mathbf{d}_\alpha)}, \quad (51)$$

where

$$\tilde{K}_j(\alpha) = \frac{1}{\pi} \sqrt{\frac{\det \tilde{\Gamma}_j}{\det \Gamma_{B,j}}} e^{-\mathbf{d}_\alpha^T \tilde{\Gamma}_{A,j} \mathbf{d}_\alpha}, \quad P_0 = \sum_{j=1}^4 C_j \tilde{K}_j(\alpha). \quad (52)$$

The coherent displacement of the output state (51) can be calculated as

$$\bar{\mathbf{d}} = \frac{1}{P_0} \sum_{j=1}^4 C_j \tilde{K}_j(\alpha) D_j \mathbf{d}_\alpha. \quad (53)$$

The symmetry of the state-preparation scheme in Fig. 3 and the teleportation protocol in Fig. 2 ensures that for the considered class of the resource entangled states (40) the matrices D_j are all proportional to the identity matrix, $D_j = d_j I$, and the effective state-dependent amplification gain can be expressed as

$$g(\alpha) = \frac{1}{P_0} \sum_{j=1}^4 C_j \tilde{K}_j(\alpha) d_j. \quad (54)$$

Following a similar procedure, one can also calculate the covariance matrix of the output amplified state (51),

$$\gamma = \frac{1}{P_0} \sum_{j=1}^4 C_j \tilde{K}_j(\alpha) \left(2\Gamma_{B,j}^{-1} + 4D_j \mathbf{d}_\alpha \mathbf{d}_\alpha^T D_j^T \right) - 4\bar{\mathbf{d}} \bar{\mathbf{d}}^T - I. \quad (55)$$

Finally, a fidelity of the output state (48) with an amplified coherent state $|g\alpha\rangle$ can be easily evaluated from the Husimi Q -function (48),

$$\mathcal{F}(\alpha) = \pi \mathcal{Q}_B(g\alpha|\beta=0) = \frac{1}{P_0} \sum_{j=1}^4 C_j \tilde{K}_j(\alpha) \sqrt{\det \Gamma_{B,j}} e^{-\mathbf{d}_\alpha^T (gI - D_j)^T \Gamma_{B,j} (gI - D_j) \mathbf{d}_\alpha}. \quad (56)$$

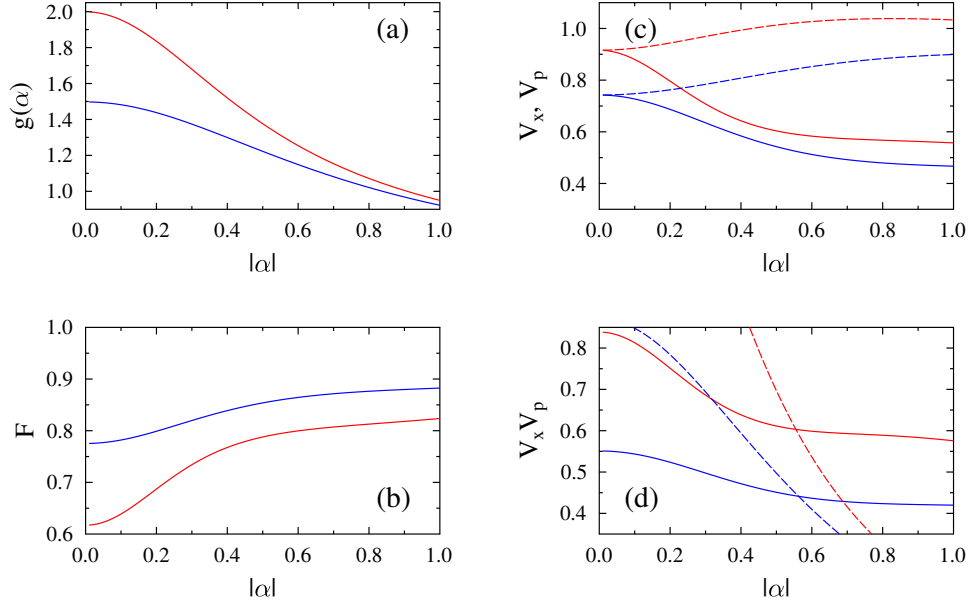


Fig. 5. Performance of realistic noiseless amplifier with parameters $\lambda = 0.5$, $T = 0.95$, $\eta_{\text{APD}} = 0.85$, $\eta_{AB} = \eta_{CD} = 0.9$, and two different values of μ yielding effective gains $g_{\text{eff}} = 1.5$ ($\mu = -0.0150$, blue curves) and $g_{\text{eff}} = 2$ ($\mu = -0.0197$, red curves). Conditioning on $\beta = 0$ is assumed. The quantities plotted are the same as in Fig. 4: (a) amplitude-dependent amplification gain; (b) fidelity of the amplified state with coherent state $|g(\alpha)\alpha\rangle$; (c) variances of amplitude and phase quadratures of the amplified state; (d) product of quadrature variances of the amplified state.

We have verified that if we consider pure input squeezed vacuum states ($\eta_{AB} = \eta_{CD} = 1$), perfect detectors with $\eta_{\text{APD}} = 1$ and tapping beam splitters with very small reflectance $R < 0.01$, then for suitable choices of λ and μ we recover the results predicted by pure state model and presented in the previous Section in Fig. 4. Let us now consider a more realistic scenario with noisy squeezed states, $\eta_{AB} = \eta_{CD} = 0.9$ and superconducting single-photon detectors with total detection efficiency $\eta = 0.85$. We assume $\lambda = 0.5$, which corresponds to 4 dB of squeezing and 4.5 dB of anti-squeezing in the resulting noisy two-mode squeezed thermal state with covariance matrix (35). The results are plotted in Fig. 5 which displays the same quantities as Fig. 4. The results are again shown for two different values of the effective gain $g_{\text{eff}} = 1.5$ and $g_{\text{eff}} = 2$. The values of squeezing strength μ that yield these gains were determined numerically and read $\mu = -0.0150$ and $\mu = -0.0197$, respectively. As expected, noisy squeezed states and imperfect single-photon detection with on-off detectors lead to reduced performance of the noiseless amplifier in comparison to the ideal pure-state scenario considered in the previous section. Most notably, the state fidelity is not a monotonously decreasing function of $|\alpha|$ but instead grows with $|\alpha|$. Note that this behavior is observed even if we consider fidelity with state $|g_{\text{eff}}\alpha\rangle$ instead of $|g(\alpha)\alpha\rangle$. Similarly, the product of quadrature variances decreases with increasing α .

To understand this behavior, we can consider setup with perfect photon number resolving detectors, vacuum in auxiliary modes C and D ($\mu = 0$), and low thermal noise with mean number of thermal photons $\bar{n}_{\text{th}} \ll 1$ in modes A and B . In this limit, the amplified coherent state can be approximately expressed as a mixture of three states $(\hat{n}+1)|\lambda\alpha\rangle$, $\alpha(\hat{n}+2)|\lambda\alpha\rangle$, and $(\hat{n}+1)\hat{a}^\dagger|\lambda\alpha\rangle$ where the probability of the last two states in the mixture is proportional to \bar{n}_{th} . For $\alpha = 0$ the state $\hat{a}^\dagger|\lambda\alpha\rangle$ becomes equal to the Fock state $|1\rangle$ that is orthogonal to the vacuum state. On the

other hand, for $\alpha \neq 0$ the state $\hat{a}^\dagger |\lambda\alpha\rangle$ has a nonzero overlap with $|\lambda\alpha\rangle$ and this overlap increases with $|\alpha|$. This explains the behavior of fidelity observed in Fig. 5(b).

In practice, a finite acceptance window for the outcomes β will be required to achieve a non-zero overall success probability of the noiseless amplification. In order to obtain analytical results, we shall again assume that the outcomes β are accepted with Gaussian probability $\exp(-|\beta|^2/\sigma^2)$. Simultaneously, we include a corrective coherent displacement proportional to β , that is applied to the output state. For teleportation with entangled Gaussian state (44), the Husimi Q -function of the resulting output single-mode state can be expressed as

$$\tilde{Q}_B(\omega_B) = \int_{\beta} Q_B(\omega_B + k\beta|\beta) e^{-\mathbf{d}_\beta^T \Sigma \mathbf{d}_\beta} d^2\beta, \quad (57)$$

where $\Sigma = \frac{1}{\sigma^2} I$ and k is a constant that determines the strength of the corrective displacement. For Gaussian Q -function (46) the integral in Eq. (57) is a Gaussian integral that can be evaluated analytically. After a lengthy but straightforward calculation we obtain

$$\tilde{Q}_B(\omega_B) = K(\alpha) \frac{\sqrt{\det \tilde{\Gamma}_B}}{\pi} e^{-(\mathbf{r}_{\omega_B} - \tilde{D} \mathbf{d}_\alpha)^T \tilde{\Gamma}_B (\mathbf{r}_{\omega_B} - \tilde{D} \mathbf{d}_\alpha)}, \quad (58)$$

where

$$K(\alpha) = \frac{1}{\sqrt{\det \Gamma_\beta}} \sqrt{\frac{\det \Gamma}{\det \tilde{\Gamma}_B}} e^{-\mathbf{d}_\alpha^T \tilde{\Gamma}_A \mathbf{d}_\alpha}. \quad (59)$$

In order to write down the formulas for the various matrices appearing in Eqs. (58) and (59) we first specify the matrix Γ_β ,

$$\Gamma_\beta = k^2 \Gamma_B + \Upsilon^T \Gamma_A \Upsilon + \Sigma + k \Upsilon^T M + k M^T \Upsilon, \quad (60)$$

and define two auxiliary matrices

$$L_\alpha = \Upsilon^T \Gamma_A \Upsilon + k M^T \Upsilon, \quad L_r = \Upsilon^T M + k \Gamma_B. \quad (61)$$

With the help of these definitions we can write down explicit formulas for the remaining matrices,

$$\begin{aligned} \tilde{\Gamma}_B &= \Gamma_B - L_r \Gamma_\beta^{-1} L_r, \\ \tilde{\Gamma}_A &= \Upsilon^T \Gamma_A \Upsilon - L_\alpha^T \Gamma_\beta^{-1} L_\alpha - (\Upsilon^T M - L_\alpha^T \Gamma_\beta^{-1} L_r) \tilde{\Gamma}_B^{-1} (M^T \Upsilon - L_r^T \Gamma_\beta^{-1} L_\alpha), \\ \tilde{D} &= -\tilde{\Gamma}_B^{-1} (M^T \Upsilon - L_r^T \Gamma_\beta^{-1} L_\alpha). \end{aligned} \quad (62)$$

If we apply the above Gaussian integration to each of the four terms in the formula (40) for the Q -function of the photon subtracted two-mode squeezed state, we obtain the final expression for the Q -function of the teleported state,

$$Q_B(\omega_B) = \frac{1}{P_{\text{tot}}} \sum_{j=1}^4 C_j \tilde{K}_j(\alpha) \frac{\sqrt{\det \tilde{\Gamma}_{B,j}}}{\pi} e^{-(\mathbf{r}_{\omega_B} - \tilde{D}_j \mathbf{d}_\alpha)^T \tilde{\Gamma}_{B,j} (\mathbf{r}_{\omega_B} - \tilde{D}_j \mathbf{d}_\alpha)}. \quad (63)$$

Here

$$\tilde{K}_j(\alpha) = \frac{1}{\sqrt{\det \Gamma_{\beta,j}}} \sqrt{\frac{\det \tilde{\Gamma}_j}{\det \tilde{\Gamma}_{B,j}}} e^{-\mathbf{d}_\alpha^T \tilde{\Gamma}_{A,j} \mathbf{d}_\alpha}, \quad P_{\text{tot}} = \sum_{j=1}^4 C_j \tilde{K}_j(\alpha). \quad (64)$$

and P_{tot} is the total success probability that is a product of the probability of state preparation P_{AB} and probability of successful conditional teleportation P_{tele} . Therefore, $P_{\text{tele}} = P_{\text{tot}}/P_{AB}$.

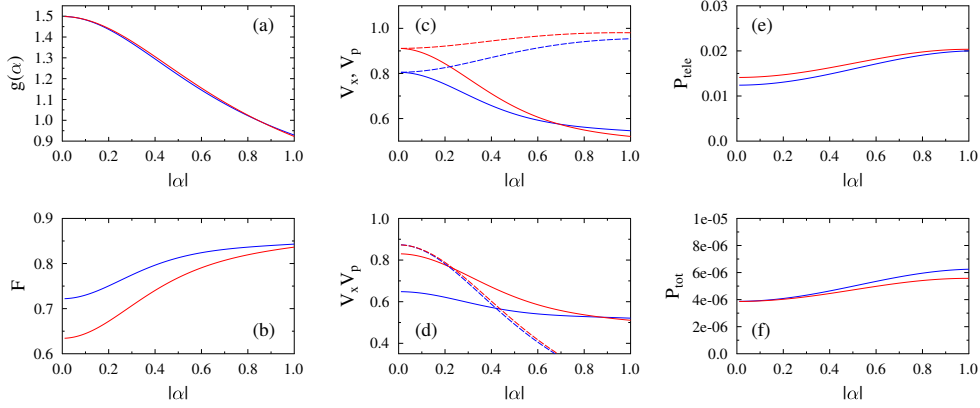


Fig. 6. Performance of realistic noiseless amplifier with parameters $\lambda = 0.5$, $\eta_{\text{APD}} = 0.85$, $\eta_{AB} = \eta_{CD} = 0.9$, $g_{\text{eff}} = 1.5$, and finite acceptance window for measurement outcomes β , $\sigma^2 = 0.08$. The blue curves indicate results for a protocol with corrective displacement: $k = 1$, $T = 0.95$, $\mu = -0.0179$. For reference, the red curves display results for a protocol without any corrective displacement: $k = 0$, $T = 0.955$, and $\mu = -0.01475$. The panels (a)-(d) display the same quantities as in Figs. 4 and 5. In the two additional panels (e,f) we plot the success probabilities P_{tele} (e), and P_{tot} (f).

The same machinery that was described above for conditioning on $\beta = 0$ can be used to calculate the various properties of the teleamplified state (63) such as the effective gain, state fidelity or quadrature variances, by employing the analogues of Eqs. (54), (55) and (56).

Figure 6 illustrates the performance of the teleportation-based noiseless amplifier for a finite acceptance window of measurement outcomes β ($\sigma^2 = 0.08$). We compare the protocols with ($k = 1$) and without ($k = 0$) corrective coherent displacement. To make a fair comparison, we choose the auxiliary squeezing parameter μ and the transmittance T of the tapping beam splitters separately for each case to achieve the same effective gain $g_{\text{eff}} = 1.5$ and the same total success probability P_{tot} for small α . We can see that the gain curves practically overlap, but the protocol with corrective displacement achieves higher fidelity and lower quadrature fluctuations of the amplified state. These results therefore clearly demonstrate the usefulness and advantage of the corrective displacement. As shown in Fig. 6(e), the success probability of the teleportation protocol itself is of the order of 1% for the parameters considered. The total success probability plotted in Fig. 6(f) is mainly reduced by small probability of preparation of the photon subtracted two-mode entangled state, here $P_{AB} \approx 3 \times 10^{-4}$. As discussed above, the state preparation can be accomplished before the teleamplification is attempted and in this sense the probability P_{tele} characterizes the probabilistic noiseless teleamplifier. However, with current technology it would not be possible to prepare the entangled state in advance and store it in a quantum memory while maintaining the required high quality of the state. Practical implementation of the protocol would therefore require simultaneous success of the conditional state preparation and teleportation, which is characterized by the total probability of success P_{tot} .

4. Conclusions

In summary, we have proposed and theoretically analyzed a scheme for noiseless quantum amplification of coherent states of light via probabilistic quantum teleportation with a suitably designed two-mode entangled state. With this approach we can implement noiseless amplifiers similar to those based on combination of conditional single photon addition and subtraction while avoiding the experimentally costly photon addition operation. Instead, the protocol requires

auxiliary two-mode squeezed vacuum states and balanced homodyne detection in addition to the conditional single photon subtraction. In its simplest version, the noiseless amplification is achieved with a two-mode squeezed vacuum with single photon subtracted from each of its modes. However, the achievable gain 2λ is limited by the available squeezing and cannot exceed 2. More control over the amplification gain can be obtained by utilizing an additional second two-mode squeezed vacuum state with low squeezing μ . With this extended scheme, arbitrary high gain (for low $|\alpha|$) is in principle achievable, but the setup may become sensitive to fluctuations of μ . Therefore, the simplest variant with $\mu = 0$ is experimentally most feasible.

The teleportation-based noiseless amplifier requires high purity squeezing to operate properly. During recent years we have witnessed tremendous progress in generation of highly pure strongly squeezed states of light, see. e.g. [42–46]. For instance, in Ref. [44], generation of squeezed state with 10 dB of squeezing and only 11 dB of anti-squeezing is reported. In our numerical simulations, we have considered a considerably lower squeezing of about 4 dB for which even higher purity is achievable. Imperfections of single photon detectors mainly limit the success probability of the protocol, while the quality of the noiseless amplifier is preserved if beam splitters with sufficiently low reflectance R are employed. With recent significant development of superconducting single photon detectors, quantum detection efficiencies exceeding 90% become available, with recently reported system detection efficiency of 98% [47]. Furthermore, the spatial or temporal multiplexing can be used to turn on-off detectors into approximate photon number resolving detectors [48], which in combination with higher reflectances R of the tapping beam splitters could significantly increase the success probability of photon subtraction while preserving high quality of the conditionally generated state.

Finally, we would like to point out that the teleportation of quantum gates can be applied also to other important elementary conditional continuous-variable quantum operations such as single photon addition. This requires as a resource state a two-mode squeezed vacuum state with a single photon subtracted from mode A,

$$\hat{a}|\Psi_{\text{TMVS}}(\lambda)\rangle = \lambda\sqrt{1-\lambda^2} \sum_{n=0}^{\infty} \sqrt{n+1}\lambda^n |n, n+1\rangle_{AB}. \quad (65)$$

For arbitrary input state $|\psi\rangle_C$, conditioning on $\beta = 0$ in the teleportation scheme in Fig. 3, the conditionally prepared output state in mode B becomes $\hat{b}^\dagger \lambda^{\hat{n}} |\psi\rangle_B$. Similarly to the teleportation-based noiseless amplification, conditioning on finite range of measurement outcomes β will unavoidably introduce some noise and imperfections into the implemented conditional operation. Nevertheless, the effective replacement of photon addition by photon subtraction can make this approach appealing for certain applications.

Funding

Czech Science Foundation (21-23120S).

Disclosure

The authors declare that there are no conflicts of interest related to this article.

References

1. S. Pandey, Z. Jiang, J. Combes, and C. M. Caves, “Quantum limits on probabilistic amplifiers,” *Phys. Rev. A* **88**(3), 033852 (2013).
2. T. C. Ralph and A. P. Lund, in *Quantum Communication Measurement and Computing*, edited by A. Lvovsky, (AIP, New York, 2009), pp. 155–160.
3. G. Y. Xiang, T. C. Ralph, A. P. Lund, N. Walk, and G. J. Pryde, “Heralded noiseless linear amplification and distillation of entanglement,” *Nat. Phot.* **4**(5), 316–319 (2010).
4. F. Ferreyrol, M. Barbieri, R. Blandino, S. Fossier, R. Tualle-Brouiri, and P. Grangier, “Implementation of a nondeterministic optical noiseless amplifier,” *Phys. Rev. Lett.* **104**(12), 123603 (2010).

5. M. A. Usuga, C. R. Muller, C. Wittmann, P. Marek, R. Filip, C. Marquardt, G. Leuchs, and U. L. Andersen, "Noise-powered probabilistic concentration of phase information," *Nature Phys.* **6**(10), 767–771 (2010).
6. A. Zavatta, J. Fiurášek, and M. Bellini, "A high-fidelity noiseless amplifier for quantum light states," *Nature Photon.* **5**(1), 52–56 (2011).
7. S. Kocsis, G. Y. Xiang, T. C. Ralph G. J. Pryde, "Heralded noiseless amplification of a photon polarization qubit," *Nature Phys.* **9**(1), 23–28 (2013).
8. C. I. Osorio, N. Bruno, N. Sangouard, H. Zbinden, N. Gisin, and R. T. Thew, "Heralded photon amplification for quantum communication," *Phys. Rev. A* **86**(2), 023815 (2012).
9. J. Fiurášek, "Engineering quantum operations on traveling light beams by multiple photon addition and subtraction," *Phys. Rev. A* **80**(5), 053822 (2009).
10. P. Marek and R. Filip, "Coherent-state phase concentration by quantum probabilistic amplification," *Phys. Rev. A* **81**(02), 022302 (2010).
11. J. Fiurášek and N. J. Cerf, "Gaussian postselection and virtual noiseless amplification in continuous-variable quantum key distribution," *Phys. Rev. A* **86**(6), 060302(R) (2012).
12. N. Walk, T. C. Ralph, T. Symul, and P. K. Lam, "Security of continuous-variable quantum cryptography with Gaussian postselection," *Phys. Rev. A* **87**(2), 020303 (2013).
13. H. M. Chrzanowski, N. Walk, S. M. Assad, J. Janoušek, S. Hosseini, T. C. Ralph, T. Symul and P. K. Lam, "Measurement-based noiseless linear amplification for quantum communication," *Nature Photon.* **8**(4), 333–338 (2014).
14. J. Y. Haw, J. Zhao, J. Dias, S. M. Assad, M. Bradshaw, R. Blandino, T. Symul, T. C. Ralph and P. K. Lam, "Surpassing the no-cloning limit with a heralded hybrid linear amplifier for coherent states," *Nature Commun.* **7**, 13222 (2016).
15. N. A. McMahon, A. P. Lund, and T. C. Ralph, "Optimal architecture for a nondeterministic noiseless linear amplifier," *Phys. Rev. A* **89**(2), 023846 (2014).
16. M. Mičuda, I. Straka, M. Miková, M. Dušek, N. J. Cerf, J. Fiurášek, and M. Ježek, "Noiseless Loss Suppression in Quantum Optical Communication," *Phys. Rev. Lett.* **109**(18), 180503 (2012).
17. N. Gisin, S. Pironio, and N. Sangouard, "Proposal for Implementing Device-Independent Quantum Key Distribution Based on a Heralded Qubit Amplifier," *Phys. Rev. Lett.* **105**(7), 070501 (2010).
18. T. C. Ralph, "Quantum error correction of continuous-variable states against Gaussian noise," *Phys. Rev. A* **84**(2), 022339 (2011).
19. H. Adnane, M. Bina, F. Albarelli, A. Gharbi, and M. G. A. Paris, "Quantum state engineering by nondeterministic noiseless linear amplification," *Phys. Rev. A* **99**(6), 063823 (2019).
20. J. Bernu, S. Armstrong, T. Symul, T. C. Ralph, and P. K. Lam, "Theoretical analysis of an ideal noiseless linear amplifier for Einstein–Podolsky–Rosen entanglement distillation," *J. Phys. B: At. Mol. Opt. Phys.* **47**(21), 215503 (2014).
21. H. Adnane and M. G. A. Paris, "Teleportation improvement by non-deterministic noiseless linear amplification," *Quantum Inf. Comput.* **19**(11-12), 0935–0951 (2019).
22. D. T. Pegg, L. S. Phillips, and S. M. Barnett, "Optical State Truncation by Projection Synthesis," *Phys. Rev. Lett.* **81**(8), 1604–1606 (1998).
23. M. S. Winnel, N. Hosseini-dehaj, and T. C. Ralph, "Generalized quantum scissors for noiseless linear amplification," *Phys. Rev. A* **102**(6), 063715 (2020).
24. J. J. Guanzone, M. S. Winnel, A. P. Lund, and T. C. Ralph, "Ideal Quantum Tele-amplification up to a Selected Energy Cut-off using Linear Optics," arXiv:2110.03172 (2021).
25. A. Ourjoumtsev, R. Tualle-Broui, J. Laurat, and Ph. Grangier, "Generating Optical Schrödinger Kittens for Quantum Information Processing," *Science* **312**(5770), 83–86 (2006).
26. J. S. Neergaard-Nielsen, B. M. Nielsen, C. Hettich, K. Molmer, and E. S. Polzik, "Generation of a Superposition of Odd Photon Number States for Quantum Information Networks," *Phys. Rev. Lett.* **97**(8), 083604 (2006).
27. K. Wakui, H. Takahashi, A. Furusawa, and M. Sasaki, "Photon subtracted squeezed states generated with periodically poled KTiOPO₄," *Opt. Express* **15**(6), 3568–3574 (2007).
28. R. Kumar, E. Barrios, C. Kupchak, and A. I. Lvovsky, "Experimental Characterization of Bosonic Creation and Annihilation Operators," *Phys. Rev. Lett.* **110**(13), 130403 (2013).
29. A. Zavatta, S. Viciani, and M. Bellini, "Quantum-to-Classical Transition with Single-Photon-Added Coherent States of Light," *Science* **306**(5696), 660–662 (2004).
30. D. Gottesman and I. L. Chuang, "Demonstrating the viability of universal quantum computation using teleportation and single-qubit operations," *Nature* **402**(6760), 390–393 (1999).
31. S. L. Braunstein and H. J. Kimble, "Teleportation of Continuous Quantum Variables," *Phys. Rev. Lett.* **80**(4), 869–872 (1998).
32. M. Fuwa, S. Toba, S. Takeda, P. Marek, L. Mišta, Jr., R. Filip, P. van Loock, J.-I. Yoshikawa, and A. Furusawa, *Phys. Rev. Lett.* **113**(22), 223602 (2014).
33. V. Parigi, A. Zavatta, M. S. Kim, and M. Bellini, "Probing Quantum Commutation Rules by Addition and Subtraction of Single Photons to/from a Light Field," *Science* **317**(5846), 1890–1893 (2007).
34. L. S. Costanzo, A. S. Coelho, N. Biagi, J. Fiurášek, M. Bellini, and A. Zavatta, "Measurement-Induced Strong Kerr Nonlinearity for Weak Quantum States of Light," *Phys. Rev. Lett.* **119**(1), 013601 (2017).
35. T. Opatrný, G. Kurizki, and D.-G. Welsch, "Improvement on teleportation of continuous variables by photon

- subtraction via conditional measurement,” *Phys. Rev. A* **61**(3), 032302 (2000).
36. H. Takahashi, J. S. Neergaard-Nielsen, M. Takeuchi, M. Takeoka, K. Hayasaka, A. Furusawa, and M. Sasaki, “Entanglement distillation from Gaussian input states,” *Nature Photon.* **4**(3), 178–181 (2010).
 37. Y. Kurochkin, A. S. Prasad, and A. I. Lvovsky, “Distillation of The Two-Mode Squeezed State,” *Phys. Rev. Lett.* **112**(7), 070402 (2014).
 38. F. Dell’Anno, D. Buono, G. Nocerino, A. Porzio, S. Solimeno, S. De Siena, and F. Illuminati, “Tunable non-Gaussian resources for continuous-variable quantum technologies,” *Phys. Rev. A* **88**(4), 043818 (2013).
 39. J. Fiurášek, R. García-Patrón, and N. J. Cerf, “Conditional generation of arbitrary single-mode quantum states of light by repeated photon subtractions,” *Phys. Rev. A* **72**(3), 033822 (2005).
 40. M. Walschaers, V. Parigi, and N. Treps, “Practical Framework for Conditional Non-Gaussian Quantum State Preparation,” *PRX Quantum* **1**(2), 020305 (2020).
 41. R. García-Patrón, J. Fiurášek, N. J. Cerf, J. Wenger, R. Tualle-Broui, and Ph. Grangier, “Proposal for a Loophole-Free Bell Test Using Homodyne Detection,” *Phys. Rev. Lett.* **93**(13), 130409 (2004).
 42. S. Suzuki, H. Yonezawa, F. Kannari, M. Sasaki, and A. Furusawa, “7dB quadrature squeezing at 860 nm with periodically poled KTiOPO₄,” *Appl. Phys. Lett.* **89**(6), 061116 (2006).
 43. M. Mehmet, S. Ast, T. Eberle, S. Steinlechner, H. Vahlbruch, and R. Schnabel, “Squeezed light at 1550 nm with a quantum noise reduction of 12.3 dB,” *Opt. Express* **19**(25), 25763-25772 (2011).
 44. H. Vahlbruch, M. Mehmet, K. Danzmann, and R. Schnabel, “Detection of 15 dB Squeezed States of Light and their Application for the Absolute Calibration of Photoelectric Quantum Efficiency,” *Phys. Rev. Lett.* **117**(11), 110801 (2016).
 45. W. Asavanant, K. Nakashima, Y. Shiozawa, J.-I. Yoshikawa, and A. Furusawa, “Generation of highly pure Schrödinger’s cat states and real-time quadrature measurements via optical filtering,” *Opt. Express* **25**(26), 32227-32242 (2017).
 46. M Mehmet and H Vahlbruch, “High-efficiency squeezed light generation for gravitational wave detectors,” *Class. Quantum Grav.* **36**(1) 015014 (2019).
 47. D. V. Reddy, R. R. Nerem, S. Woo Nam, R. P. Mirin, and V. B. Verma, “ Superconducting nanowire single-photon detectors with 98% system detection efficiency at 1550 nm,” *Optica* **7**(12), 1649-1653 (2020) .
 48. E. Meyer-Scott, C. Silberhorn, and A. Migdall, “Single-photon sources: Approaching the ideal through multiplexing featured,” *Rev. Sci. Instrum.* **91**(4), 041101 (2020).